The effects of laser absorption on direct-drive capsule experiments at OMEGA

E. S. Dodd, J. F. Benage, G. A. Kyrala, D. C. Wilson, F. J. Wysocki et al.

Citation: Phys. Plasmas **19**, 042703 (2012); doi: 10.1063/1.3700187
View online: http://dx.doi.org/10.1063/1.3700187
View Table of Contents: http://pop.aip.org/resource/1/PHPAEN/v19/i4
Published by the American Institute of Physics.

The effects of laser absorption on direct-drive capsule experiments at OMEGA

E. S. Dodd,[1] J. F. Benage,[1] G. A. Kyrala,[1] D. C. Wilson,[1] F. J. Wysocki,[1] W. Seka,[2] V. Yu. Glebov,[2] C. Stoeckl,[2] and J. A. Frenje[3]
[1]*Los Alamos National Laboratory, Los Alamos, New Mexico 87545, USA*
[2]*Laboratory for Laser Energetics, University of Rochester, Rochester, New York 14623-1299, USA*
[3]*Plasma Science and Fusion Center, Massachusetts Institute of Technology, Cambridge, Massachusetts 02139, USA*

(Received 15 September 2011; accepted 15 March 2012; published online 5 April 2012)

The yield of an inertial confinement fusion capsule can be greatly affected by the inclusion of high-Z material in the fuel, either intentionally as a diagnostic or from mixing due to hydrodynamic instabilities. To validate calculations of these conditions, glass shell targets filled with a D_2 and ^{3}He fuel mixture were fielded in experiments with controlled amounts of pre-mixed Ar, Kr, or Xe. The experiments were fielded at the OMEGA laser [T. R. Boehly *et al.*, Opt. Commun. **133**, 495 (1997)] using 1.0 ns square laser pulses having a total energy 23 kJ and direct drive illumination of shells with an outer diameter of ~925 μm and a thickness of ~5 μm. Data were collected and compared to one-dimensional integrated models for yield and burn-temperature measurements. This paper presents a critical examination of the calculational assumptions used in our experimental modeling. A modified treatment of laser-capsule interaction improves the match to the measured scattered laser light and also improves agreement for yields, burn-temperatures, and the fuel compression as measured by the ratio of two yields. Remaining discrepancies between measurement and calculation will also be discussed. © *2012 American Institute of Physics*. [http://dx.doi.org/10.1063/1.3700187]

INTRODUCTION

Inertial confinement fusion (ICF) uses the ablation of spherical shells to drive shocks that implode and compress a fuel mixture to condition where thermonuclear burn (TN-burn) is possible.[1] Experiments aimed at using ICF to achieve ignition, or self-heating of the fuel from the TN-reactions, are now underway at the National Ignition Facility.[2] The implosion dynamics and yield of an ICF capsule can be greatly affected by the inclusion of shell material in the fuel, which has motivated studies of the hydrodynamic stability of an imploding shell starting with the earliest work.[1] However, studying the physics of how a quantity of mixed shell material impacts performance is just as important. Thus, the integrated models used to design and interpret ICF implosions must be validated against experimental data for this total process. However, the validation can initially be divided into the two separate physical processes that both must be modeled correctly. The first is the amount of material transport between the fuel and the shell from turbulent mixing, and the second is the effects of the mixed material on the plasma conditions of the fuel region during TN-burn. This paper examines only the latter process.

The validation work presented herein will compare the results from as-shot calculations to data from direct-drive capsule implosions fielded at the OMEGA laser.[3] The capsules will be described in detail below but were glass shells filled with a fuel mixture of deuterium and ^{3}He, as shown in Fig. 1. Variations in this base target were then made to study the impact of mix on burn physics. Validation of the TN-burn is accomplished by including a known amount of a pre-mixed material into the fuel and is done in this case by adding various amounts of Ar, Kr, or Xe to the gas-fill. This methodology is valid when enough pre-mix is included to minimize the effects of natural turbulent mixing, and the plasma conditions are determined dominantly by the amount of pre-mix.

Previously published modeling of these implosions[4,5] identified a discrepancy between experimental and calculated yields using a 1-D integrated model described below. As the fraction of Kr added to the fuel is increased, the capsule yield is reduced, which both calculation and experiment qualitatively agree on. However, the amount needed to significantly reduce the yield is different, for a gas-fill containing 0.05 atm of Kr, the measured yield is approximately a factor of six smaller than the calculated yield. Similar results were reported in Ref. 4 for Ar and Xe. These three yield discrepancies are summarized in Fig. 2. Here, the amount of pre-mix needed to reduce the yield by 50% has been plotted as a function of the atomic number (Z) of the added pre-mix, and which shows that the reduction threshold scales as $f(Z) \sim Z^{-2}$. Also, shown are unreported yield reduction results due to He pre-mix, which gave results similar to those reported by Rygg *et al.*[6] and Herrmann *et al.*[7] The work presented here will concentrate on the fills containing only Kr since the results of Fig. 2 show that our conclusions do not change qualitatively for other gas fills. The differences reported in Ref. 4 were calculated using XSN LTE inline opacity calculations and were even greater for calculations using XSN non-LTE. It was also shown in Ref. 4 that the neutron reaction history for capsules with Ar pre-mix deviated from those without, and the time when the deviation occurs coincides with the outgoing fuel shock striking the converging shell after rebounding from the capsule center.

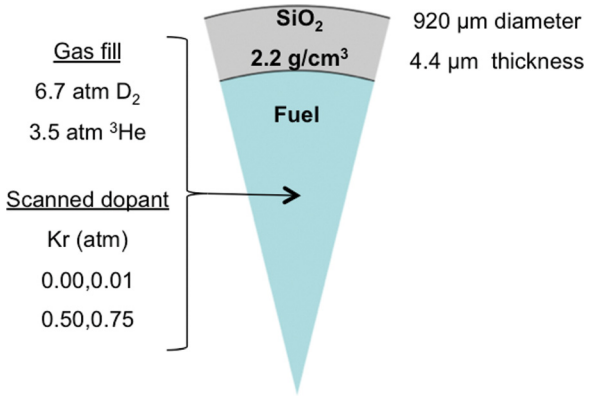

FIG. 1. The capsules used were SiO_2 shells with a typical outer diameter of 925 ± 15 μm, a thickness of 5.0 ± 0.5 μm, and an average density of 2.2 g/cm^3. They were filled with a fuel mixture, which typically included 6.7 atm of deuterium and 3.3 atm of ^{3}He. The base target was varied by including a known amount of a pre-mixed Kr gas in the fuel in the amounts of 0.00 atm (base), 0.01 atm, 0.05 atm, and 0.75 atm.

In this paper, we present a critical examination of the laser absorption process in our capsule calculations, which were motivated by laser absorption data that were not initially available at the time Ref. 4 was written. This work uses data from two more recent capsule implosions to determine two multipliers, the electron-thermal flux limiter and a multiplier on the incident laser energy, such that the code calculation reproduces the measured absorption. These new multipliers are then applied to the calculations for the set of Kr pre-mixed capsules reported in Ref. 4, which leads to better agreement with experiment. These improvements include: some improvement to the D(D,^{3}He)n yield ($Y_{DD\text{-}n}$), an improvement to the calculated compression (or ρR) measured by the ratio of neutron yields ($Y_{DD\text{-}n}/Y_{DT\text{-}n}$), and improvement to the calculated ion temperature. However, these improvements fail to remediate the previously reported yield degradation discrepancy. We will also discuss possible explanations and work done to eliminate some of the explanations.

EXPERIMENTAL SETUP

As mentioned in the Introduction, the data for validation were acquired with direct-drive capsule experiments at the OMEGA laser. The capsules were SiO_2 shells[8,9] with a typical outer diameter of 925 ± 15 μm, a thickness of 5.0 ± 0.5 μm, and an average density of 2.2 g/cm^3. The shells were filled with a fuel mixture, which typically included 6.7 atm of deuterium and 3.3 atm of ^{3}He, as shown in Fig. 1. The base target was varied to provide test data for capsule calculations by including a known amount of a pre-mixed Kr gas in the fuel. The work presented here concentrates on the shells containing only Kr in the amounts of 0.00 atm (base), 0.01 atm, 0.05 atm, and 0.75 atm. While the value of 0.01 atm of Kr produces the results similar to the base case, the higher values of Kr significantly alter the capsule performance.

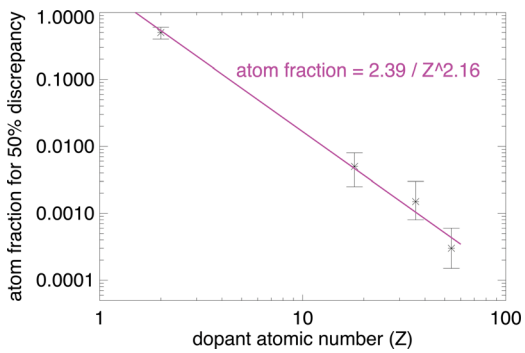

FIG. 2. The amount of pre-mix needed to reduce the yield by 50% has been measured and plotted as a function of atomic number, Z, for the data described in Ref. 4. The data include pre-mixed He, Ar, Kr, and Xe and show that the yield reduction threshold scales as $f(Z) \sim Z^{-2}$.

The targets were irradiated in the 60-beam OMEGA laser facility[3] using 1-ns square pulses (SG1018) with a total incident laser energy of ~23 kJ. Optimum beam smoothing was applied using SG4 phase plates[10] and 1-THz smoothing by spectral dispersion (SSD)[11] generating 4th-order super-Gaussian intensity profiles on target. The spot size on target allows for ~8% of the laser energy to spill around the target.

A significant difference between this paper and Ref. 4 is the use of scattered laser data. This light is measured using full-aperture back-scatter stations (FABS) that record the scattered light through the focusing lenses of beams 25 and 30. Time-integrated scattered light energy and time-resolved scattered light spectra are measured in two wavelength regions, one near the incident wavelength (351 nm ± 1 nm) and the other between 400 nm and 720 nm. The former measures unabsorbed light and stimulated-Brillouin scattering (SBS), while the latter corresponds to stimulated-Raman scattering (SRS, 400 to 700 nm, not observed in these experiments) and the two-plasmon decay instability (TPD, 702 ± 20 nm).[12] The time-dependent incident and scattered light powers are recorded on each shot using streak cameras from which the time-dependent laser-absorption into the shell can be obtained.[13] The total fraction of absorbed laser-energy is used to compare with hydrodynamic simulations. For the 60-beam OMEGA irradiation geometry, the scattered light distribution for standard spherical implosion targets has been determined to be close to isotropic.[13] Typical experimental data are shown in Fig. 3 and are discussed in the Calculation Setup section.

Cross-beam energy transfer has been identified as a significant energy loss mechanism for direct-drive implosion experiments.[14] Combined ray trace and hydrodynamic simulations have shown that the resulting scattered energy distribution still remains very close to isotropic as observed experimentally.[13] This is a result of the symmetry built into the OMEGA irradiation facility. The simulated spectral characteristics of cross-beam energy transfer deviate significantly from the simulated spectra for purely refractive (unabsorbed) scattered light spectra. The spectral characteristics of the latter are a result of temporally changing coronal plasma conditions including the implosion of the target shell during irradiation.

A number of other diagnostics were fielded on each shot to measure the various outputs from the ICF implosions. Neutron diagnostics were used to record the neutron yields from the D(D,^{3}He)n and D(T,α)n reactions and the plasma ion temperature during TN-burn. Tritium was not initially present in the gas-fill and was bred through the D(D,T)p

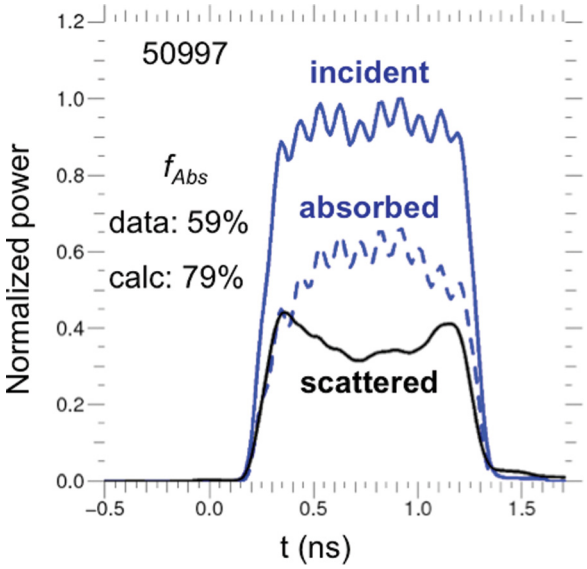

FIG. 3. Data from OMEGA shot 50 997 are shown for the time-dependent incident power (blue solid line), scattered power (solid black line), and the difference of these two signals (dashed blue line). This difference is the measurement of the laser absorption. For shot 50 997, the measured fraction of total incident energy to absorbed energy was ~60%, while ~80% was calculated when the full laser power was initially used in the calculation.

reaction; however, enough secondary D-T neutrons were produced to be measureable. The time-dependent neutron reaction rate was measured using the neutron temporal diagnostic (NTD).[15] The proton yield and the time-integrated spectra were recorded using wedge-range filters for the D(^{3}He,α)p reaction, and the corresponding time-dependent reaction rate was recorded with the proton temporal diagnostic (PTD).[16] The yields from D(D,T)p are not measured directly and are only determined indirectly through the D-T reaction listed above.

Time-gated x-ray framing camera images and both time-integrated and time-dependent x-ray spectra were also collected for each shot. X-ray spectra are important when experiments have intentionally included trace gases, such as Ar (Ref. 17) and Kr,[18] in the fuel, and which are used to diagnose spectroscopically the fuel temperature and density. The case of 0.01 atm of Kr was used to measure the electron temperature, and the results of which were discussed elsewhere.[19] X-ray diodes were also fielded to measure the emission in various energy bands for the thermal radiation (DANTE) and hot-electron generated hard-x-rays (HXRD).

CALCULATION SETUP

The calculations of the experiments presented in this paper were all performed using a one-dimensional integrated model of the laser-absorption, implosion, and TN-burn. The hydrodynamics of the implosion are performed on a Langrangian mesh, which includes a dynamic model for turbulent mixing.[20] The radiation transfer equation is solved using multi-group flux-limited diffusion, and in-line calculation of the opacity is performed using non-LTE XSN. The energy released by burn is deposited in the material; however, for these experiments, it is too little to affect the capsule hydrodynamics. The burn reactions are used instead to calculate the synthetic diagnostics, which are post-processed for each run. These diagnostics include: two primary yields, $Y_{DD\text{-}n}$ and $Y_{D3He\text{-}p}$, and one secondary yield, $Y_{DT\text{-}n}$; the burn-weighted ion-temperature; and the time-dependent neutron reaction rate. All synthetic diagnostics include a detector response. Two other physical processes, laser absorption and electron thermal transport, are discussed in more detail below.

The laser was modeled using a ray-based method that accounts for refraction of the laser light through the ablated material and can account for energy not being fully absorbed by the capsule. The absorption process was modeled as classical inverse-bremsstrahlung integrated and deposited zonally into the electron internal energy. The model also included a so-called "dump-all" to account for resonance absorption near the critical surface, which can generate a second thermal distribution of hot electrons. However, for blue light with $\lambda = 351$ nm and an average intensity of $I_0 \sim 1 \times 10^{15}$ W/cm^2, the hot electrons would have a temperature of $T_e \sim 10$ keV and a number fraction of $f \sim 0.01$.[21] For this reason, we claim that resonance absorption is unimportant to these implosions and have set the dump-all to zero. Any light reflected at the critical surface is included in the directly measured scattering and is thus accounted for by the absorption measured. Calculations that match the integrated absorption data should, therefore, account for the reflections at the critical surface. Ponderomotive steepening of the electron density near the critical surface is also possible but can also be assessed[22] and is again unimportant to these implosions. This laser model does not account for any nonlinear scattering processes such as SRS or SBS, which are generally not observed in these experiments except possibly for cross-beam energy transfer. And, if scattering is present, then it must be taken into account in an *ad hoc* manner such as a multiplier used to reduce the incident energy. The total amount of, and time-history for, the laser absorption can also be post-processed for comparison with experimental results. As mentioned above, these data were not initially available but did become available during the on-going experimental campaign. An example is shown in Fig. 3 for OMEGA shot 50 997, which shows the time-dependent incident power (blue solid line) and scattered power (solid black line). The difference of these two signals (dashed blue line) is the measurement of the laser absorption averaged over 4π, and what an integrated calculation should match. For shot 50 997, the measured total absorbed energy as a fraction of the incident energy was ~60%, while ~80% was calculated using the full laser power. We will proceed by applying only a fraction of the incident laser power, m, in the calculations.

Direct-drive capsule implosions are sensitive to the amount of laser energy absorbed by the shell, but this has typically been an unknown quantity. The kinetic energy, or velocity, of the imploding shell is just as useful and could be characterized by the time to reach peak compression. An integrated model is thus important for modeling an implosion, since it links the laser absorption and capsule energy through physics. The amount of absorbed energy is sensitive to the rate at which the ablation front propagates into the shell, which is modeled by diffusive electron thermal conduction and hydrodynamic motion. However, it has long

been known that an arbitrary flux-limiter is needed to model the process properly.[23] Adjusting the flux-limiter, f_e, to match the timing of the implosion is thus the typical way to adjust a calculation to get the energy of the shell correct. The measured timing typically comes from the time of peak neutron production rate, which for an implosion where most of the yield is due to compression burn should correspond to a time near peak compression. However, setting the flux-limiter to match the time for peak neutron production will get the kinetic energy of the shell correct only if all of the burn physics in the integrated model is also correct. Here, we consider the burn physics to include the complexity of spatial energy transport and energy exchange among the ions, electrons and radiation, and not simply the thermonuclear reaction rate. The purpose of our capsule experiments is to validate the physics used to model TN-burn but using the method just described couples burn physics and laser absorption physics.

Electron thermal conduction in a capsule has typically been modeled in the diffusion approximation with a theoretically calculated coefficient[24] and is the method used in our integrated model. In radiation hydrodynamics, the penetration of thermal (or Planckian) radiation into cold material can also be modeled with a diffusion equation. A standard solution describing this process was found by Marshak[25] for the case of a static-material and a temperature-dependent opacity. However, it was shown that this solution deposits too much energy into the material and the radiation front calculated with diffusion outruns the front for a transport solution.[26] Reducing the deposited laser energy reduces the electron temperature near the ablation front, and thus by analogy with Marshak will also reduce the speed of the thermal front. Therefore, using a multiplier on laser energy to account for scattering will also affect the electron thermal conduction. Differences between diffusion and more detailed modeling of electron conduction have long been known and have motivated the development of physics-based non-local heat transport models.[27–32] Two of these models (Refs. 30 and 31) have recently been shown to improve the modeling of hohlraum energetics[33] and shock timing.[34] We presently lack non-local electron conduction, as well as a physics-based model for cross-beam energy transfer. However, the approach taken in the Parameter Study section calculates the absorption close enough to assess to what extent the yield discrepancy is due to inaccurately modeled implosion drive. This is a valid approach, because our model agrees with the measured scattered light.

PARAMETER STUDY

While adjusting the flux-limiter allows the time of peak neutron production to be matched well, typically no other measured quantity can be simultaneously matched by this method. However, by varying a second parameter, or multiplier, on some other process, one would expect that it might be possible to match two measured quantities. The current computational study is thus a two-parameter scaling using many 1-D integrated code calculations to map out the capsule dynamics and performance. The first varied parameter is the electron conduction flux-limiter (f_e), which is justified for the reasons already discussed. The second varied parameter is a multiplier applied to the incident laser energy to account for any unknown losses (m), but which also affects the conduction. Laser absorption in a capsule happens over a finite spatial extent and not at a single point or surface. We have elected to use a single multiplier that behaves as a transmission coefficient at the problem boundary, and since there is uncertainty in the physics process responsible, there is also uncertainty in the spatial extent affected. This methodology is valid, because our intent is to understand the dependence of capsule dynamics on absorbed laser energy, and not the underlying physics of a specific scattering process.

The two-parameter study for a given capsule uses 288 calculations (24 values of f_e by 12 values of the m) and collects six synthetic diagnostics, which includes the absorbed energy, particle yields, burn-temperature, and time of peak neutron–production. Once a table of these values is created, a measured quantity can then be compared to its synthetic equivalent, and a contour line generated in the two-parameter space along which calculation matches experiment for that particular quantity. Two capsule implosions were chosen to perform this study, OMEGA shots 50 997 and 51 483, and an example of this type output is shown in Fig. 4. Both capsules were similar to the base case (no Kr) depicted in Fig. 1. However, shot 50 997 had a modified fuel ratio (3.7 atm D_2 and 7.0 atm ^{3}He), and shot 51 483 used pure D_2 and a reduced laser pulse length (0.6 ns). The examples in Fig. 4 are from shot 51 483 but are qualitatively similar for either of the two-parameter scans. Fig. 4(a) shows the case for a yield, $Y_{DD\text{-}n}$, and Fig. 4(b) the time where the neutron rate equals 10^{-2} times the peak rate and approximately when the shock reflects from the center. The colors, as shown in the color bar, represent the calculated quantity and how it varies over the two-parameter space. Over-plotted is a white contour line, which is the set of points where the synthetic quantity agrees with experimental measurement.

As mentioned six synthetic quantities were generated for the entire parameter scan and the corresponding six contours generated for shot 50 997 are shown in Fig. 5. This shot is the closest to the Kr-doped implosions of interest in terms of laser pulse and capsule geometry for which the laser absorption was also measured. The six measured quantities (contours) shown are the ion burn-temperature (cyan solid line); time for peak neutron production (black solid line); the total absorbed laser energy (solid green line); and the three particle-yields $Y_{DD\text{-}n}$ (solid blue line), $Y_{DT\text{-}n}$ (dashed blue line), and $Y_{D3He\text{-}p}$ (red dashed line). As mentioned, any of the six measured quantities can be matched in a calculation by picking a flux-limiter and laser-energy multiplier, (f_e, m), along the appropriate contour. There are also several points in the two-parameter space where the calculation agrees simultaneously with two measured quantities but no point where all measured quantities are matched. While this method cannot account for all discrepancies between calculation and experiment, it does, however, suggest an alternate way, or ways, to calculate the energy of an imploding shell and make reductions in the discrepancies.

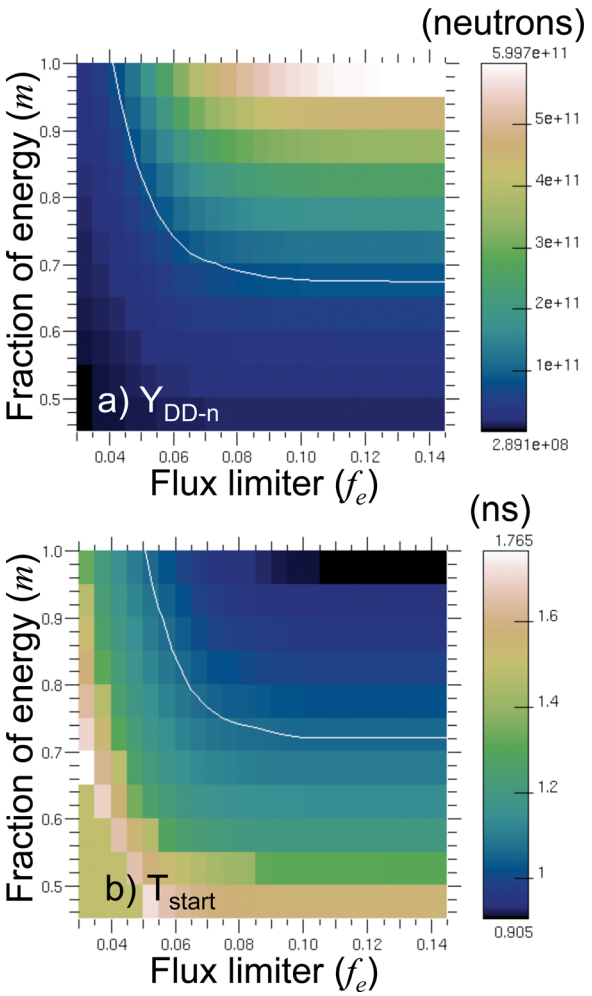

FIG. 4. Examples are plotted from the two-parameter scan of shot 51 483. (a) shows the case for a yield, $Y_{DD\text{-}n}$, and (b) the time where the neutron rate equals 10^{-2} times the peak rate (T_{start}) and is approximately when the shock reflects from the center of the target. The colors, as shown in the color bar, represent the calculated quantity. Over-plotted is a white contour line, which is the set of points where the synthetic quantity agrees with experimental measurement.

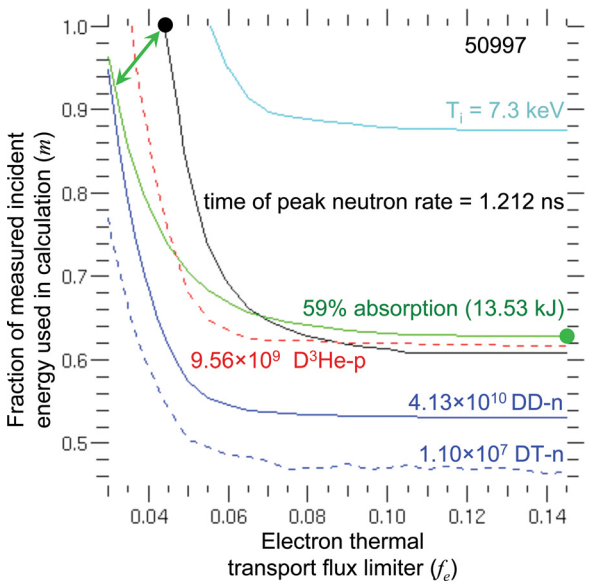

FIG. 5. The six measured quantities (contours) for shot 50 997 shown are as follows: the ion burn-temperature (cyan solid line); neutron bang time (black solid line); the total absorbed laser energy (solid green line); and the three particle yields $Y_{DD\text{-}n}$ (solid blue line), $Y_{DT\text{-}n}$ (dashed blue line), and $Y_{D3He\text{-}p}$ (red dashed line). Any measured quantity can be matched in a calculation by picking a point, (f_e, m), along the appropriate contour. The large dots mark the multipliers used for the old (black) and new (green) calculations and are discussed in more detail in the text.

The contention of the previous discussion was that using the flux-limiter to match the neutron bang time convolves laser absorption with TN-burn and should be avoided when validating a burn model. To illustrate our new method and discuss differences with previous work, two points have also been marked in Fig. 5 with large dots colored black ($f_e = 0.045$, $m = 1.00$) and green (0.145, 0.63). A horizontal line for any given laser energy multiplier in Fig. 5 varies only the flux-limiter and corresponds to setting the capsule energy by the previous method when using the full incident laser energy $m = 1.00$. The point along this line where the calculation reproduces the measured time of peak neutron production is equivalent to the result from the standard method for setting the shell energy and is marked with the black dot. However, because the total laser energy absorbed has been measured, any point along the green curve will match the total energy of the shell (kinetic and internal) independently from the burn model. This line does not intersect the black dot, which means that setting the timing solely with the flux-limiter leads to an incorrect total shell energy. This discrepancy is marked using a double arrow near the upper-left-hand corner of Fig. 5. The two-parameter variation actually leads to a degenerate solution, where any point along the green contour should match the total shell energy. It should be noted that the large flux-limiters, i.e., $f_e \geq 0.1$, are equivalent to not using a limiter, and this limit may be chosen using the combination of flux-limiter and energy multiplier marked by the green dot, $f_e = 0.145$ and $m = 0.63$. This point is physically equivalent to assuming that electron thermal conduction using diffusion is correct and any discrepancy in shell energy is due to incorrectly modeled laser propagation, absorption, and scattering. Notice that the green point in Fig. 5 also nearly matches two other measured quantities, the measured proton yield and the time of peak neutron production. We contend that this is an appropriate alternative to the traditional method of setting f_e to match solely the time of peak neutron production rate. This point defines our new model and will be used for the as-shot Kr-filled capsule calculations in the Calculations section of the paper.

CALCULATIONS

The original purpose of these experiments was to validate capsule burn calculations in the presence of a known contaminant, but Ref. 4 reported discrepancies between calculation and experiment. New calculations of these experiments will be presented in this section using the modified flux-limiter and laser energy from the previous sections and compared with the previous calculations. Fig. 6 shows the neutron yield $Y_{DD\text{-}n}$ as a function of Kr-fraction in the fuel for three sets of points: the experimentally measured yields (black circles), the previous calculations (green triangles), and the new calculations with improved laser absorption (blue diamonds). There is an overlap between the three sets

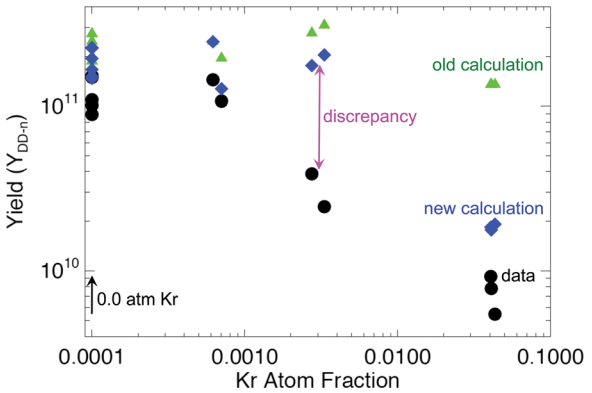

FIG. 6. The neutron yield $Y_{DD\text{-}n}$ is plotted as a function of Kr-fraction in the fuel for three sets of points: the experimentally measured yields (black circles), the previous calculations (green triangles), and the new calculations (blue diamonds). There is an overlap between the three sets of points for Kr-fractions of 0.0 and ~0.001 (*n.b.* the x-axis is logarithmic and a 0.0 Kr-fraction has been offset to 0.0001).

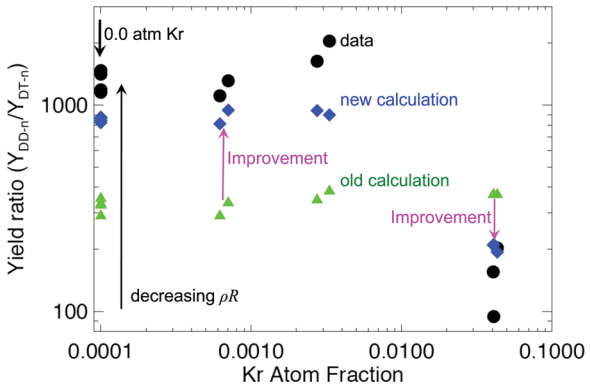

FIG. 7. The ratio, $Y_{DD\text{-}n}/Y_{DT\text{-}n}$, is plotted as a function of the fuel Kr-fraction for the same three sets of data and simulations in Fig. 6. The ratio used in this plot, $Y_{DD\text{-}n}/Y_{DT\text{-}n}$, increases with decreasing ρR, and thus less compressed capsules appear towards the top of the plot and more compressed capsules near the bottom.

of points for Kr-fractions of 0.0 and ~0.001 (*n.b.* the x-axis is logarithmic and a 0.0 Kr-fraction has been offset to 0.0001). But, there is only a modest improvement in the yields calculated for the base and lowest level of Kr when the improved modeling of the shell energy is used. For these cases, the ratio of measured-to-calculated yields (Y_{meas}/Y_{calc}) is only changed by a small amount in the new calculations for lower amounts of Kr, i.e., $Y_{meas}/Y_{calc} \sim 0.5$ in the original case and $Y_{meas}/Y_{calc} \sim 0.7$ for the new calculation, and as previously mentioned, the calculations include a model for hydrodynamic mixing. The new calculations for 0.0 and 0.01 atm Kr give $Y_{meas}/Y_{calc} \sim 0.3$ without the mix model. The inclusion of the dynamic mix model does not significantly alter the yield results at the highest level of Kr, which is consistent with the largest amounts of Kr dominating over the dynamic mix. More importantly, at a Kr-fraction of 0.003 the outstanding discrepancy remains, and both sets of calculations over predict the yield by a large factor, ~5 to 10. However, there has been improvement for the largest amounts of Kr dopant (at a fraction of ~0.04). Where the previous calculations over predicted yield by more than a factor of 10, the new results are only a factor of a few higher, $Y_{meas}/Y_{calc} \sim 2$ to 3. The reason for this improvement will be discussed in the context of improved agreement between other synthetic data and the measured data.

The yield ratio of primary reaction neutrons to secondary reaction neutrons, $Y_{DD\text{-}n}/Y_{DT\text{-}n}$, is used as a measure of capsule compression, or ρR, in ICF implosions. Capsules containing deuterium in the fuel but lacking tritium initially will breed tritium through one branch of the D-D reaction. The bred tritium starts with an energy 1.01 MeV and will undergo a D-T reaction after energy loss due to the surrounding fuel plasma.[35] This ratio is plotted in Fig. 7 as a function of the fuel Kr-fraction for the same set of data and simulations as in Fig. 6. There is a substantial change to the calculation results when using the improved laser absorption model. The ratio used in this plot, $Y_{DD\text{-}n}/Y_{DT\text{-}n}$, increases with decreasing ρR, and thus less compressed capsules appear towards the top of the plot and more compressed capsules near the bottom. Fig. 7 shows that in the previous calculations ρR was larger than the measured value for lower fractions of Kr (i.e., the green triangles appear below the black circles). The calculations also did not match the measured functional dependence on Kr-fraction. There is a measured increase in ρR for large amounts of Kr, which can happen for two reasons: an increased electron density from the Kr-dopant, and the Kr-dopant increases the coupling to radiation and leads to increased compression. For either process, the increased ρR will increase the probability of a D-T reaction for the bred energetic T. The new calculations using the corrected laser absorption more closely match the measured ρR and its dependence on Kr-fraction.

Accurate calculation of the fuel density and temperature present in any ICF experiment is necessary to calculate the correct reaction rates and particle yields. The yields shown in Fig. 6 and fuel compressions shown in Fig. 7 both show an increased agreement between calculated and measured results at the highest Kr-fraction for the modified laser absorption. Some improvement to the burn-weighted ion-temperature was also achieved and is shown in Fig. 8 for the same set of data and simulations. At the highest Kr-fraction of 0.04, the original calculated temperatures were substantially different from the measurements in Ref. 4. While this

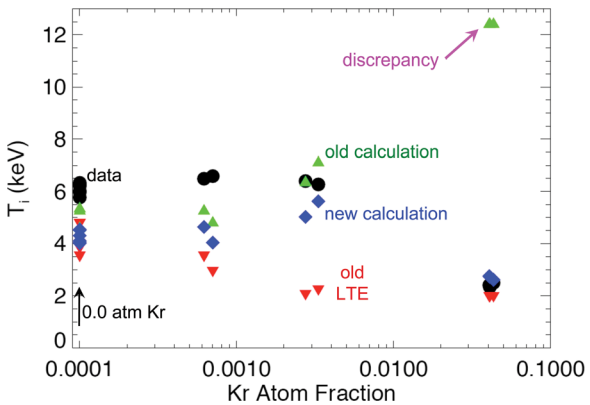

FIG. 8. The burn-weighted ion-temperature is shown for the same set of data and simulations as in Figs. 6 and 7. At the highest Kr-fraction level of 0.04, the original calculated temperatures were substantially different from the measurements in Ref. 4.

is the most likely reason for the yield discrepancy at the highest Kr-fraction, it was only the case for calculations using non-LTE XSN opacities. However, the calculations using the improved laser absorption are in strong agreement with the measured temperatures for this amount of Kr. The new calculations again use non-LTE XSN but are more consistent with the LTE XSN calculations of Ref. 4. However, for the other three levels of Kr in fuel, there is no substantial difference between the two calculation sets, and the burn temperature discrepancy remains even with the improved laser absorption.

DISCUSSION AND SUMMARY

The work presented in this paper has clearly shown that using newly available laser absorption measurements based on scattered laser power led immediately to the improvements in our calculations of capsule performance. This not only shows the importance of correct drive modeling but also the importance of the underlying method used to evaluate implosion modeling. However, Kr-fraction dependent discrepancies remain between calculated and measured performance, which implies that some other physics is not correct in our integrated models.

Some modifications to the burn physics (e.g., use of detailed configuration accounting (DCA) inline opacity calculations and modification to the electron-ion equilibration rates) were tried but did not yield changes consistent with the observed discrepancies. The recent work by Amendt *et al.*[36] is also considered as a possible explanation. The results from Ref. 36 suggest that our discrepancy could be explained by the presence of baro-diffusion in these implosions. We have not fully evaluated this phenomenon for our experiments, which will be left for future research.

The method presented in this paper is simply an empirical fitting of two *ad hoc* multipliers through comparisons of experimental data to synthetic diagnostic outputs generated from the calculations. However, the preferred method is to identify the physical process responsible for the low modeled-absorption, and add a physics-based model of the process to the integrated model of the capsule implosion. A number of scattering processes are possible in direct-drive capsule implosions, but the most likely candidate is crossed-beam energy transfer.[37] A model for this process for direct–drive capsules has been recently developed by Igumenshchev *et al.*[38] but was unpublished during the course of this work. An additional two-parameter scaling with a multiplier on the laser focal spot size was performed but not included in this paper. Although an increased spot size can qualitatively reproduce Fig. 5, it requires a radial increase of $\sim$2.5 and is much larger than the effective spot size increase of Ref. 38. Given this fact, we feel that applying a multiplier to the incident energy is an expeditious way to assess capsule performance in the presence of increased scattering without detailed modeling of the underlying scattering process. The results presented show that the improved physical modeling of the laser-plasma interactions and electron thermal conduction are needed in our integrated capsule calculations but are not expected to change the conclusions of this paper regarding the modeling of TN-burn.

ACKNOWLEDGMENTS

The authors would like to acknowledge useful conversations with Nelson Hoffman and Manolo Sherrill. The authors also wish to thank the staff at LLE who run the OMEGA laser facility and the staff of General Atomics who fabricated the targets. This work was supported by the U.S. Department of Energy, and operated by Los Alamos National Security LLC under Contract Nos. DE-AC52-06NA25396 and LA-UR-11-05291.

[1]J. Nuckolls, L. Wood, A. Thiessen, and G. Zimmerman, Nature (London) **239**, 139 (1972).
[2]E. I. Moses, R. N. Boyd, B. A. Remington, C. J. Keane, and R. Al-Ayat, Phys. Plasmas **16**, 041006 (2009).
[3]T. R. Boehly, D. L. Brown, R. S. Craxton, R. L. Keck, J. P. Knauer, J. H. Kelly, T. J. Kessler, S. A. Kumpan, S. J. Loucks, S. A. Letzring, F. J. Marshall, R. L. McCrory, S. F. B. Morse, W. Seka, M. M. Soures, and C. P. Verdon, Opt. Commun. **133**, 495 (1997).
[4]D. C. Wilson, G. A. Kyrala, J. F. Benage, Jr., F. J. Wysocki, M. A. Gunderson, W. J. Garbett, V. Yu. Glebov, J. Frenje, B. Yaakobi, H. W. Herrmann, J. H. Cooley, L. Welser-Sherrill, C. J. Horsfield, and S. A. Roberts, J. Phys.: Conf. Ser. **112**, 022015 (2008).
[5]W. J. Garbett, S. James, G. A. Kyrala, D. C. Wilson, J. F. Benage, F. J. Wysocki, M. A. Gunderson, J. Frenje, R. Petrasso, V. Yu. Glebov, and B. Yaakobi, J. Phys.: Conf. Ser. **112**, 022016 (2008).
[6]J. R. Rygg, J. A. Frenje, C. K. Li, F. H. Seguin, R. D. Petrasso, J. A. Delettrez, V. Yu. Glebov, V. N. Goncharov, D. D. Meyerhofer, S. P. Regan, T. C. Sangster, and C. Stoeckl, Phys. Plasmas **13**, 056702 (2006).
[7]H. W. Herrmann, J. R. Langenbrunner, J. M. Mack, J. H. Cooley, D. C. Wilson, S. C. Evans, T. J. Sedillo, G. A. Kyrala, S. E. Caldwell, C. S. Young, A. Nobile, J. Wermer, S. Paglieri, A. M. McEvoy, Y. Kim, S. H. Batha, C. J. Horsfield, D. Drew, W. Garbett, M. Rubery, V. Yu. Glebov, S. Roberts, and J. A. Frenje, Phys. Plasmas **16**, 056312 (2009).
[8]A. Nikroo, F. H. Elsner, D. G. Czechowicz, J. Gibson, S. E. Grant, A. L. Greenwood, M. L. Hoppe, D. Hysband, B. W. McQuillan, W. J. Miller, J. M. Ponteandolfo, D. A. Steinman, R. B. Stevens, K. R. Schulkz, and M. Takagi, "Capsule production and development for ICF experiments," General Atomics Report No. GA-A23228, 1999.
[9]G. A. Kyrala, J. F. Benage, M. A. Gunderson, D. C. Wilson, K. A. Klare, J. Frenje, R. Petrasso, B. Yaakobi, V. Glebov, W. Garbett, and S. James, "Post-shot report high Z implosions March 1st 2006," Los Alamos National Laboratory Report No. LA-UR-06-5467, 2006; G. A. Kyrala, "Pre-shot report for January 18th 2007 Hi-Z experiments," Los Alamos National Laboratory Report No. LA-UR-07-0301, 2007.
[10]F. J. Marshall, J. A. Delettrez, R. Epstein, R. Forties, R. L. Keck, J. H. Kelly, P. W. McKenty, S. P. Regan, and L. J. Waxer, Phys. Plasmas **11**, 251 (2004).
[11]S. Skupsky and R. S. Craxton, Phys. Plasmas **6**, 2157 (1999).
[12]W. Kruer, "The physics of laser-plasma interaction," in *Frontiers in Physics*, edited by D. Pines (Addison-Wesley, Redwood City, CA, 1988), Vol. 73, Chaps. VII and VIII, pp. 73–94.
[13]W. Seka, D. H. Edgell, J. P. Knauer, J. F. Myatt, A. V. Maximov, R. W. Short, T. C. Sangster, C. Stoeckl, R. E. Bahr, R. S. Craxton, J. A. Delettrez, V. N. Goncharov, I. V. Igumenshchev, and D. Shvarts, Phys. Plasmas **15**, 056312 (2008).
[14]D. H. Edgell, W. Seka, J. A. Delettrez, R. S. Craxton, V. N. Goncharov, I. V. Igumenshchev, J. F. Myatt, A. V. Maximov, R. W. Short, T. C. Sangster, and R. E. Bahr, Bull. Am. Phys. Soc. **54**, 145 (2009).
[15]R. A. Lerche, D. W. Phillion, and G. L. Tietbohl, Rev. Sci. Instrum. **66**, 933 (1995).
[16]J. A. Frenje, C. K. Li, F. H. Séguin, J. Deciantis, S. Kurebayashi, J. R. Rygg, R. D. Petrasso, J. Delettrez, V. Yu. Glebov, C. Stoeckl, F. J. Marshall, D. D. Meyerhofer, T. C. Sangster, V. A. Smalyuk, and J. M. Soures, Phys. Plasmas **11**, 2798 (2004).
[17]B. Yaakobi, S. Skupsky, R. L. McCrory, C. F. Hooper, H. Deckman, P. Bourke, and J. M. Soures, Phys. Rev. Lett. **44**, 1072 (1980); S. P. Regan, J. A. Delettrez, R. Epstein, P. A. Jaanimagi, B. Yaakobi, V. A. Smalyuk, F. J. Marshall, D. D. Meyerhofer, W. Seka, D. A. Haynes, I. E. Golovkin, and C. F. Hooper, Phys. Plasmas **9**, 1357 (2002).
[18]B. Yaakobi, R. Epstein, C. F. Hooper, Jr., D. A. Haynes, Jr., and A. Su, J. X-Ray Sci. Technol. **6**, 172 (1996).

[19]G. A. Kyrala, D. C. Wilson, J. F. Benage, Jr., M. Gunderson, K. Klare, J. Frenje, R. Petrasso, W. Garbett, S. James, V. Glebov, and B. Yaakobi, High Energy Density Phys. **3**, 163 (2007).
[20]G. Dimonte, Phys. Plasmas **7**, 2255 (2000).
[21]D. W. Forslund, J. M. Kindel, K. Lee, E. L. Lindman, and R. L. Morse, Phys. Rev. A **11**, 679 (1975).
[22]K. Lee, D. W. Forslund, J. M. Kindel, and E. L. Lindman, Phys. Fluids **20**, 51 (1977).
[23]R. C. Malone, R. L. McCrory, and R. L. Morse, Phys. Rev. Lett. **34**, 721 (1975).
[24]Y. T. Lee and R. M. More, Phys. Fluids **27**, 1273 (1984).
[25]R. E. Marshak, Phys. Fluids **1**, 24 (1958).
[26]D. Mihalas and B. Weibel-Mihalas, *Foundations of Radiation Hydrodynamics* (Dover, 1999), Sec. 103, pp. 547–557.
[27]J. F. Luciani, P. Mora, and J. Virmont, Phys. Rev. Lett. **51**, 1664 (1983).
[28]J. R. Albritton, E. A. Williams, I. B. Bernstein, and K. P. Swartz, Phys. Rev. Lett. **57**, 1887 (1986).
[29]E. M. Epperlein and R. W. Short, Phys. Fluids B **3**, 3092 (1991).
[30]G. P. Schurtz, Ph. D. Nicolai, and M. Busquet, Phys. Plasmas **7**, 4238 (2000).
[31]V. N. Goncharov, T. C. Sangster, P. B. Radha, R. Betti, T. R. Boehly, T. J. B. Collins, R. S. Craxton, J. A. Delettrez, R. Epstein, V. Yu. Glebov, S. X. Hu, I. V. Igumenshchev, J. P. Knauer, S. J. Loucks, J. A. Marozas, F. J. Marshall, R. L. McCrory, P. W. McKenty, D. D. Meyerhofer, S. P. Regan, W. Seka, S. Skupsky, V. A. Smalyuk, J. M. Soures, C. Stoeckl, D. Shvarts, J. A. Frenje, R. D. Petrasso, C. K. Li, F. Seguin, W. Manheimer, and D. G. Colombant, Phys. Plasmas **15**, 056310 (2008).
[32]W. Manheimer, D. Colombant, and V. Goncharov, Phys. Plasmas **15**, 083103 (2008).
[33]M. D. Rosen, H. A. Scott, D. E. Hinkel, E. A. Williams, D. A. Callahan, R. P. J. Town, L. Divol, P. A. Michel, W. L. Kruer, L. J. Suter, R. A. London, J. A. Harte, and G. B. Zimmerman, High Energy Density Phys. **7**, 180 (2011).
[34]T. R. Boehly, V. N. Goncharov, W. Seka, M. A. Barrios, P. M. Celliers, D. G. Hicks, G. W. Collins, S. X. Hu, J. A. Marozas, and D. D. Meyerhofer, Phys. Rev. Lett. **106**, 195005 (2011).
[35]T. E. Blue and D. B. Harris, Nucl. Sci. Eng. **77**, 463 (1981); H. Azechi, N. Miyanaga, R. O. Stapf, K. Itoga, H. Nakaishi, M. Yamanaka, H. Shiraga, R. Tsuji, S. Ido, K. Nishihara, Y. Izawa, T. Yamanaka, and C. Yamanaka, Appl. Phys. Lett. **49**, 555 (1986).
[36]P. Amendt, O. L. Landen, H. F. Robey, C. K. Li, and R. D. Petrasso, Phys. Rev. Lett. **105**, 115005 (2010).
[37]P. Michel, S. H. Glenzer, L. Divol, D. K. Bradley, D. Callahan, S. Dixit, S. Glenn, D. Hinkel, R. K. Kirkwood, J. L. Kline, W. L. Kruer, G. A. Kyrala, S. Le Pape, N. B. Meezan, R. Town, K. Widmann, E. A. Williams, B. J. MacGowan, J. Lindl, and L. J. Suter, Phys. Plasmas **17**, 056305 (2010).
[38]I. V. Igumenshchev, D. H. Edgell, V. N. Goncharov, J. A. Delettrez, A. V. Maximov, J. F. Myatt, W. Seka, A. Shvydky, S. Skupsky, and C. Stoeckl, Phys Plasmas **17**, 122708 (2010).